White Matter Microstructure and Atypical Visual Orienting in 7 Month-Olds at Risk for Autism

Journal:	*The American Journal of Psychiatry*
Manuscript ID:	AJP-12-09-1150.R2
Manuscript Type:	Article
Date Submitted by the Author:	n/a
Complete List of Authors:	Elison, Jed; California Institute of Technology, Humanities and Social Sciences Paterson, Sarah; Children's Hospital of Philadelphia, Department of Pediatrics Wolff, Jason; University of North Carolina at Chapel Hill, Carolina Institute for Developmental Disabilities Reznick, J.; University of North Carolina at Chapel Hill, Psychology Sasson, Noah; University of Texas at Dallas, School of Behavioral and Brain Sciences Gu, Hongbin; University of North Carolina at Chapel Hill, Carolina Institute for Developmental Disabilities; University of North Carolina at Chapel Hill, Psychiatry Botteron, Kelly; Washington University, Psychiatry Dager, Stephen; University of Washington, Radiology Estes, Annette; University of Washington, Speech and Hearing Sciences Evans, Alan; McGill University, McConnell Brain Imaging Centre Gerig, Guido; University of Utah, Scientific Computing and Imaging Institute Hazlett, Heather; University of North Carolina, Psychiatry; UNC, Carolina Institute for Developmental Disabilities Schultz, Robert; Children's Hospital of Philadelphia, Center for Autism Research; University of Pennsylvania, Pediatrics Styner, Martin; University of North Carolina at Chapel Hill, Psychiatry Zwaigenbaum, Lonnie; University of Alberta, Pediatrics Piven, Joseph; University of North Carolina at Chapel Hill, Department of Psychiatry
Keywords:	Autism - AJP0006, Brain Imaging Techniques - AJP0068, Child Psychiatry - AJP0102

Word Count (abstract = 248, text = 4052, references = 1154, tables & figures = 734)
Tables (2); Figures (5)

WHITE MATTER MICROSTRUCTURE AND ATYPICAL VISUAL ORIENTING IN 7 MONTH-OLDS AT RISK FOR AUTISM

Jed T. Elison, PhD*[1,5], Sarah J. Paterson, PhD[6], Jason J. Wolff, PhD[1], J. Steven Reznick, PhD[1,3], Noah J. Sasson, PhD[7], Hongbin Gu, PhD[1,2], Kelly N. Botteron, MD[8], Stephen R. Dager, MD[9], Annette M. Estes, PhD[10], Alan C. Evans, PhD[11], Guido Gerig, PhD[12], Heather C. Hazlett, PhD[1,2], Robert T. Schultz, PhD[6], Martin Styner, PhD[1,2,4], Lonnie Zwaigenbaum, MD[13], Joseph Piven, MD*[1,2] for the IBIS Network[†]

[1]Carolina Institute for Developmental Disabilities, University of North Carolina at Chapel Hill
[2]Department of Psychiatry, University of North Carolina at Chapel Hill
[3]Department of Psychology, University of North Carolina at Chapel Hill
[4]Department of Computer Science, University of North Carolina at Chapel Hill
[5]Division of Humanities and Social Sciences, California Institute of Technology
[6]Center for Autism Research, Children's Hospital of Philadelphia, University of Pennsylvania
[7]School of Behavioral and Brain Sciences, The University of Texas at Dallas
[8]Department of Psychiatry, Washington University in St. Louis
[9]Department of Radiology, University of Washington
[10]Department of Speech and Hearing Sciences, University of Washington
[11]Montreal Neurological Institute, McGill University
[12]Scientific Computing and Imaging Institute, University of Utah
[13]Department of Pediatrics, University of Alberta
[†]The Infant Brain Imaging Study (IBIS) Network is an NIH funded Autism Center of Excellence project and consists of a consortium of 7 universities in the U.S. and Canada. Clinical Sites: University of North Carolina: J. Piven (IBIS Network PI), H.C. Hazlett, J.C. Chappell; University of Washington: S. Dager, A. Estes, D. Shaw; Washington University: K. Botteron, R. McKinstry, J. Constantino, J. Pruett; Children's Hospital of Philadelphia: R. Schultz, S. Paterson; University of Alberta: L. Zwaigenbaum; Data Coordinating Center: Montreal Neurological Institute: A.C. Evans, D.L. Collins, G.B. Pike, P. Kostopolous, S. Das; Image Processing Core: University of Utah: G. Gerig; University of North Carolina: M. Styner; Statistical Analysis Core: University of North Carolina: H. Gu; Genetics Analysis Core: University of North Carolina: P. Sullivan, F. Wright.

Aspects of this work were presented at the International Meeting for Autism Research (IMFAR): Toronto, ON, Canada; May 17 -19, 2012.
***Correspondence**: Jed T. Elison, PhD, Division of Humanities and Social Science, California Institute of Technology, 1200 E. California Blvd., MC 228-77, Pasadena, CA 91125 (jelison@caltech.edu) or Joseph Piven, MD, Carolina Institute for Developmental Disabilities, University of North Carolina, Chapel Hill, NC 27599-7255 (jpiven@med.unc.edu).

Disclosure & Acknowledgments: Dr. Evans is cofounder of and holds equity in Biospective, Inc., a company that performs image analysis for pharmaceutical companies; he has also received consulting fees from Johnson & Johnson and Pfizer within the last 36 months. Dr. Schultz reports receiving CME funding from Shire Pharmaceuticals, advisory panel funding from Seaside Therapeutics, and advisory panel funding from Roche. All other authors report no financial relationships with commercial interests. This research was supported by grants awarded to J.P. from NIH/NICHD (Autism Center of Excellence R01 #HD055741, #HD055741-S1; IDDRC, P30 #HD03110; and T32 HD40127), Autism Speaks, and the Simons Foundation. J.T.E. was supported by an NRSA award (5-T32-HD007376) from NICHD and aspects of this work contributed to his PhD dissertation. Further support was provided by the National Alliance for Medical Image Computing (NA-MIC), funded by the NIH through grant U54 EB005149.

Abstract

Objective: To determine whether specific patterns of oculomotor functioning and visual orienting characterize 7 month-old infants later classified with an autism spectrum disorder (ASD) and to identify the neural correlates of these behaviors.

Method: Ninety-seven infants contributed data to the current study (16 high-familial risk infants later classified with an ASD, 40 high-familial risk infants not meeting ASD criteria (high-risk-negative), and 41 low-risk infants). All infants completed an eye tracking task at 7 months and a clinical assessment at 25 months; diffusion weighted imaging data was acquired on 84 infants at 7 months. Primary outcome measures included average saccadic reaction time in a visually guided saccade procedure and radial diffusivity (an index of white matter organization) in fiber tracts that included corticospinal pathways and the splenium and genu of the corpus callosum.

Results: Visual orienting latencies were increased in seven-month-old infants who later express ASD symptoms at 25 months when compared with both high-risk-negative infants ($p = 0.012$, $d = 0.73$) and low-risk infants ($p = 0.032$, $d = 0.71$). Visual orienting latencies were uniquely associated with the microstructural organization of the splenium of the corpus callosum in low-risk infants, but this association was not apparent in infants later classified with ASD.

Conclusions: Flexibly and efficiently orienting to salient information in the environment is critical for subsequent cognitive and social-cognitive development. Atypical visual orienting may represent an early-emerging prodromal feature of ASD, and abnormal functional specialization of posterior cortical circuits directly informs a novel model of ASD pathogenesis.

White Matter Microstructure and Atypical Visual Orienting in

7 Month-Olds at Risk for Autism

Developmental models of autism spectrum disorders (ASD) suggest that atypical or biased visual attention patterns in the first year of life could directly contribute to the emergence of the characteristic social-cognitive deficits (1). Indeed, many of the early behavioral markers associated with later emerging ASD, specifically orienting to name, responding to bids for joint attention, spontaneous gaze to faces, and making eye contact (2-4), implicate behaviors associated with flexibly allocating attentional resources to salient or biologically relevant information in the environment.

Selective attention refers to the process by which information is channeled, filtered, and/or enhanced for further processing in higher-order neural systems. It has long been recognized that selective attention shapes the development of adaptive cognitive function (5). Although the neural circuitry of selective attention has been comprehensively delineated in adults (6-10) and selective attention's role in social-cognition continues to be elucidated (10-11), the precise circuitry that underlies selective visual attention during infancy is unknown. Characterizing the neural correlates of visual attention during infancy may inform our understanding of cortical specialization, as experience with specific categories of information may sculpt neural circuits and enhance processing efficiency (12).

The specialized perception, processing, and evaluation of social information readily observable in typically developing individuals remain a source of impairment in individuals with ASD. Navigating the subtle complexities of social dynamics often requires rapid, flexible, and efficient information processing. But prior to the actual processing of social information, flexibly orienting gaze and visual attention to the most salient or biologically relevant information in the environment is essential. We reasoned that a deficit in visual orienting during infancy could constrain typical developmental processes leading to specialization with social information, thereby contributing to the emergence of social-communication deficits related to a later diagnosis of ASD. Nine to ten-month-old infants at high-familial risk for developing autism (n=16) have been reported to show increased visual orienting latencies when compared to low-risk, typically developing infants (13). Another study reported that visual orienting latencies

measured in a high-risk cohort at 12 months (n=27) correlated with autism symptom severity at 24 months (2). While these studies informed our current hypotheses, critical questions remain as to whether compromised visual orienting behavior is specific to infants who later express ASD, and if so, how early can this behavioral pattern be detected.

We employed a well validated, visually guided saccade task (the gap overlap paradigm) to examine saccade latencies in 2 conditions that represent visual orienting (overlap condition) and oculomotor efficiency (gap condition), respectively. We also used diffusion tensor imaging to delineate specific white matter fiber tracts hypothesized to be associated with these behaviors. A recent diffusion tensor imaging study reported a unique association between orienting and the splenium of the corpus callosum in adults (9). ~~Additionally, individual differences in saccade latency (in the gap/overlap paradigm) have been mapped to individual differences in the amplitude of the pre-saccadic spike potentials over central-parietal regions in 12-month-olds (14).~~ The splenium is the most posterior sector of the corpus callosum and projects to striate and extrastriate visual areas and to portions of the posterior parietal cortex, including Brodmann's area 7 (14), a cortical target implicated in sensorimotor programming (15). This tract may function in part as transitional connectivity between extrastriate visual areas and the dorsal frontoparietal and ventral frontoparietal orienting networks identified in adults (10).

Saccadic eye movements that represent oculomotor efficiency, as operationalized in this context, result from temporary inhibition of fixation neurons in the rostral pole of the superior colliculus and disinhibition of the saccade generating circuit mediated in part by the reticular formation in the brain stem (16). Therefore, we hypothesized that individual differences in the organization of white matter fiber bundles projecting from the brain stem to cortical targets, namely corticospinal tracts, would be associated with individual differences in oculomotor efficiency. Finally, we examined the genu of the corpus callosum as a control tract. The genu projects to frontal association areas associated with voluntary, goal directed attentional operations (9).

In the current study, we sought to determine whether 7-month-olds later classified as expressing ASD symptoms exhibit different patterns of oculomotor efficiency and visual orienting when compared

with other similar-aged infants. We then examined the neural correlates of task-based behavioral performance and whether the patterns of brain-behavior associations differed between groups.

Methods

Sample

This study took place in the context of an ongoing Autism Center of Excellence (ACE) Network study prospectively investigating longitudinal brain and behavioral trajectories in high-familial-risk infant siblings of children with ASD and low-risk control infants. Infants were considered at high-familial-risk if they have a biological sibling diagnosed with an ASD. All infants were enrolled at approximately 6 months of age and participated in a comprehensive behavioral assessment and brain imaging protocol around the 6, 12, and 24 month age intervals (actual chronological age of the child at the time of the visit lags slightly behind the target visit stages). The data used to investigate the hypotheses in the current study include behavioral, imaging, and eye tracking data from the initial 6 month visit stage and clinical assessment data from the 24 month visit stage. Participants in this study were assessed at the University of North Carolina at Chapel Hill and the Children's Hospital of Philadelphia sites. The research protocol was approved by the Internal Review Boards at both sites and written informed consent was obtained from parents after the study was fully explained. Upon study entry, exclusion criteria for both high-familial-risk and low-familial-risk (hereafter high-risk and low-risk) children included the following: 1) history or physical signs of known genetic conditions or syndromes; 2) significant medical or neurological conditions affecting growth, development, or cognition or sensory impairments such as significant vision or hearing loss; 3) birth weight less than 2000 grams and/or gestational age of less than 36 weeks, a history of significant perinatal adversity, exposure in-utero to neurotoxins (including alcohol, illicit drugs, selected prescription medications); 4) a contraindication for MRI; 5) a predominant home language other than English; 6) having been adopted; and 7) a family history of a 1° degree relative with an intellectual disability (only for low-risk), psychosis, schizophrenia, bipolar disorder. Low-risk infants were excluded for a family history of a first or second degree relative with autism or if the low-risk proband (older sibling) showed symptoms of ASD measured with the Social Communication

Questionnaire (17). Clinical diagnosis was corroborated in the proband of high-risk infants with the Autism Diagnostic Interview – Revised (18).

Infants were included in this study if they participated in the eye tracking protocol during the 6 month visit and had an outcome classification at 24 months. 113 infants were eligible for the current study according to these criteria. 14 infants did not complete a sufficient number of trials in the eye tracking task (low-risk = 8, high-risk = 6) and were excluded from subsequent analyses. These infants did not differ in age ($p = 0.477$) or developmental level ($p = 0.827$) from those infants included in subsequent analyses. Two infants were enrolled as low-risk but subsequently exceeded the Autism Diagnostic Observation Schedule threshold for an ASD and were excluded from the current analyses. The final sample included 97 infants. See Table 1 for characterization of the sample.

Clinical Assessment

Primary cognitive assessments during the 6 month visit stage included the Mullen Scales of Early Learning (19). ASD classification was made during the 24 month visit stage with the Autism Diagnostic Observation Scale (ADOS; ref 20). The ADOS was used to maximize reliable classification of ASD symptoms and was conducted and scored by experienced, research-reliable clinicians. A total of 97 infants completed the experimental task and were categorized into three groups based on risk status and ASD classification on the ADOS including low-risk infants (n = 41), high-risk infants who did not meet ASD criteria on the ADOS (high-risk-negative, n = 40), and high-risk infants who met ADOS criteria for an ASD (high-risk-ASD, n = 16). Seven low-risk, 4 high-risk-negative, and 2 high-risk-ASD participants did not contribute valid imaging data, but contributed valid eye tracking data, yielding 84 infants with valid imaging data and eye tracking data.

[Insert Table 1]

Eye Tracking Procedure

We measured overt, stimulus driven orienting during visually guided saccade trials in which the timing of the fixation offset and target-stimulus onset was manipulated to examine 1) oculomotor efficiency and 2) visual orienting (see Figure 1). Eye movements were recorded with corneal-reflection

binocular eye-tracking equipment (Tobii models 1750 and x120, recordings sampled at 50 and 60 Hz respectively). The primary dependent measure was latency to initiate a saccade away from the center image (or center of the display in the gap condition) in the correct direction of the target. Average saccadic latency in the gap condition represents raw oculomotor efficiency. The offset of the fixation stimulus primes the oculomotor system and results in the temporary inhibition of fixation neurons in the rostral pole of the superior colliculus and disinhibition of the saccade generating circuit mediated in part by the reticular formation in the brain stem (16). Individual differences in average gap latency stem in part from the relative computational efficiency of these circuits; hence we refer to "oculomotor efficiency" when describing saccadic latencies in the gap condition. Average saccadic latency in the overlap condition encapsulates a combination of oculomotor responding and attentional orienting (disengaging and shifting attention). Overlap latencies are consistently longer than gap latencies, likely resulting from 1) additional processing demands supported by the lateral intraparietal area (16;28-29) and 2) the absence of the fixation offset priming effects. We refer to saccadic latencies in the overlap condition as "visual orienting," as this concept subsumes both attentional and oculomotor components.

The current study was primarily concerned with domain-general response patterns as there is evidence to suggest that 6 month-old infants who later develop ASD show similar patterns of 'gaze to faces' and 'gaze to objects' as 6 month-olds who do not develop ASD (4). Therefore, we included a variety of complex stimuli (parametrically varied among central and peripheral locations) that included 10 distinct faces and 10 distinct objects. Trials were counterbalanced with no direction (i.e., left or right), condition (i.e., gap or overlap), or central or peripheral stimulus type respectively (i.e., faces or objects) occurring on more than 3 consecutive trials. For more information on the procedure, see the supplemental information.

[Insert Figure 1]

Imaging Protocol

Diffusion weighted images were acquired during natural sleep on a Siemens 3T TIM Trio scanner equipped with a 12-channel headcoil using the following parameters: Field-of-View = 190 mm, 75

transversal slices, slice thickness = 2 mm isotropic, 2x2x2mm^3 voxel resolution, TR = 12800 ms, TE = 102 ms, b-values of 0 to 1000 sec/mm^2, 25 gradient directions, and 4-5 minute scan time. Image data were screened for motion and common artifacts using DTIprep software (www.nitrc.org/projects/dtiprep), and expert raters manually removed scans with residual artifacts.

Computational Anatomy Mapping

Image registration proceeded in two steps (30). First, linear affine registration of baseline images was applied to the structurally weighted T2 atlas using B-spline registration and normalized mutual information (31). Second, a large deformation diffeomorphic metric mapping transformation was applied for unbiased, deformable atlas building (32). The procedure related each individual dataset to the study-specific atlas template via a nonlinear, invertible transformation, providing a precise match between the reference atlas and individual image data. Tensor maps were calculated from each dataset using weighted least squares estimation (33), and transformed into the atlas space with tensor re-orientation by a finite strain approach (34). DTI tensor images were transformed and averaged using the Riemannian and log-Euclidean frameworks (35), resulting in the final 3D average tensor atlas.

Segmentation and Parameterization of Fiber Tracts

Deterministic tractography was performed by manually drawing seed label maps for the splenium and genu of the corpus callosum and bilateral corticospinal tracts (broadly defined as corticospinal pathways passing through the posterior limb of the internal capsule) based on methods described previously (36) using 3D Slicer (www.slicer.org; see Figure 2). Seed spacing was set at 1mm and proceeded bidirectionally with a linear measure stopping value of 0.1. Extracted fiber tracts were processed for spurious or incomplete streamlines using software developed in-house (FiberViewer; www.ia.unc.edu/dev/). Fiber tracts were converted to binary regions-of-interest and mapped to individual datasets to generate scalar diffusion measures (i.e., radial diffusivity, axial diffusivity, and fractional anisotropy) along each fiber bundle, from which mean values were derived. We initially chose to focus on radial diffusivity as there have been reports linking this metric to myelination (37), and the relative myelin content is thought to support rapid and efficient signal transmission (38) and therefore efficient

information processing. However, there is evidence to suggest that the density and diameter of axons in a given fiber tract, in addition to myelin content, affect the diffusion of water molecules perpendicular to the primary eigenvector of a fiber tract (39). Radial diffusivity was calculated in the conventional manner as the mean of the second and third eigenvalues [$(\lambda_{2,} + \lambda_3)/2$]. To supplement analyses of radial diffusivity reported below, we also examined axial diffusivity and the composite index, fractional anisotropy. The results from these additional analyses are reported in the supplemental information document.

[Insert Figures 2a and 2b]

Results

According to a Fisher's exact test, the sex ratio did not significantly differ between groups, p = 0.427. The three groups of children did not statistically differ in age during the initial 6 month visit stage, $F(2,94) = 0.51$, $p = 0.604$; age during the 24 month clinical visit stage, $F(2,94) = 1.57$, $p = 0.215$; nonverbal developmental quotient as measured by the Mullen Scales of Early Learning during the 6 month visit stage, $F(2,94) = 0.08$, $p = 0.919$; or the standardized score on the visual reception subscale of the Mullen Scales of Early Learning during the 6 month visit stage, $F(2, 94) = 0.10$, $p = 0.904$.

A multivariate ANOVA that included gap latency and overlap latency as dependent variables and risk status (low-risk, high-risk-negative, and high-risk-ASD) as the independent variable was statistically significant, Wilks Λ (.879), $F(4,188) = 3.097$, $p = 0.017$, $\eta_p^2 = .062$. The statistical model also revealed a significant main effect of risk status on both gap latencies $F(2, 94) = 3.14$, $p = 0.048$, $\eta_p^2 = 0.063$ and overlap latencies $F(2, 94) = 3.42$, $p = 0.037$, $\eta_p^2 = 0.068$. Planned post-hoc comparisons revealed that the high-risk-ASD group showed significantly longer gap latencies than the low-risk group ($p = 0.025$, d = 0.71), and that the high-risk-negative group did not significantly differ from the low-risk ($p = 0.074$, d = 0.41) or high-risk-ASD ($p = 0.362$, $d = 0.26$) groups. Considering the overlap condition, the high-risk-ASD group showed significantly longer latencies than both the high-risk-negative group ($p = 0.012$, d = 0.73) and the low-risk group ($p = 0.032$, $d = 0.71$). The low-risk and high-risk-negative groups showed

statistically equivalent overlap latencies ($p = 0.598$, $d = 0.12$). See Figure 3 for graphical representation and Table 2 for full characterization of performance on the gap/overlap task.

[Insert Table 2]

[Insert Figure3]

Next, we tested the specificity of the association between average saccadic latency in the gap condition and white matter fiber tracts that transmit information to and from the brain stem (i.e., the corticospinal tract), and the association between average saccadic latencies in the overlap condition and the splenium of the corpus callosum. To accomplish this, we also examined the association between the saccadic latencies and the genu of the corpus callosum, to confirm the specificity of any observed association with splenium and/or the corticospinal tracts. We report results using radial diffusivity and provide additional data on fractional anisotropy and axial diffusivity when relevant.

In low-risk infants [n = 34, average age in weeks (standard deviation) = 31.0(3.5)], hierarchical multiple regression analyses (Figure 4) verified that performance in the two conditions of the gap/overlap procedure was related to dissociable white matter fiber tracts. Average latency in the gap condition accounted for a significant portion of variance in radial diffusivity in the left corticospinal tract ($\Delta R^2 = 0.486$, $p < 0.001$) beyond the contribution of age and overlap latency. Average latency in the overlap condition accounted for a significant portion of variance in radial diffusivity in the splenium beyond the contribution of age and gap latency ($\Delta R^2 = 0.297$, $p = 0.001$). Gap latencies did not account for a significant portion of variance in the splenium ($\Delta R^2 = 0.010$, $p = 0.860$) and overlap latencies did not account for significant portion of variance in the left corticospinal tract ($\Delta R^2 = 0.016$, $p = 0.475$). There was no association between latencies in the gap/overlap procedure and our control tract, the genu of the corpus callosum (p's > 0.211, see Supplemental Figure 2). All of these patterns remain when we examine fractional anisotropy and axial diffusivity (see Supplemental Information) with the exception that gap latencies did not account for a significant portion of variance in fractional anisotropy in the left corticospinal tract ($\Delta R^2 = 0.097$, $p = 0.076$) beyond the effect of age and overlap latency. However, the trend toward statistical significance is consistent with the results from radial and axial diffusivity.

[Insert Figures 4a and 4b]

Considering the pattern of results in the overlap condition (high-risk-ASD > high-risk-negative = low-risk), alongside the finding that overlap latencies (visual orienting) are associated with the splenium in low-risk infants, directly informed the final question: do the functional properties of the splenium explain the increased overlap latencies observed in infants who later express ASD symptoms? We employed a General Linear Model that included overlap latencies as the dependent variable and group, radial diffusivity in the splenium, and a group X splenium interaction term as independent variables. Group status moderated the association between white matter microstructure in the splenium and overlap latencies. The overall model was significant, $F(5,78) = 2.82$, $p = 0.021$. Additionally, the results revealed a main effect of group, $F(2, 78) = 4.16$, $p = 0.019$, $\eta_p^2 = 0.096$, as well as a significant group X splenium interaction, $F(2, 78) = 4.53$, $p = 0.014$, $\eta_p^2 = 0.104$. Average radial diffusivity in the splenium did not differ between groups ($p = 0.428$). The significant interaction indicates that the association between brain and behavior varies by group. The simple slope for the low-risk group significantly differed from the simple slope for the high-risk-ASD group ($t = -2.95$, $p = 0.004$). The simple slope for the high-risk-negative group did not significantly differ from the low-risk group ($t = -1.63$, $p = 0.107$) or the high-risk-ASD group ($t = -1.33$, $p = 0.186$). See graphical representation in Figure 5. This pattern of results and specifically the significant difference in simple slopes between the low-risk group and the high-risk-ASD group is corroborated by analyses conducted with axial diffusivity (see the Supplemental Information). For additional results regarding the moderating effect of group status on the association between gap latencies and the left corticospinal tract, see Supplemental Figures 3 & 5.

[Insert Figure 5]

Discussion

One underlying theme of this study was to elucidate mutually informative findings regarding both typical and atypical development processes. This is among the first studies to characterize an association between specific white matter fiber tracts and specific behavioral patterns in typically developing infants, an approach that lends itself to inferences regarding functional circuits during infancy. Our results

suggest that among typically developing infants, individual differences in visual orienting are associated with individual differences in white matter microstructure of the splenium of the corpus callosum. Visual orienting latencies were not related to the microstructure of the corticospinal tracts, nor were they associated with the anterior segment of the corpus callosum, the genu. Supporting our claims of specificity, oculomotor efficiency, as represented by saccadic latencies in the gap condition, were significantly associated with white matter microstructure in the corticospinal tracts, but not associated with white matter in the splenium or the genu of the corpus callosum. This pattern is consistent with studies examining DTI-related associations with attentional operations in adults (9), as well as behavioral evidence from a rare infant hemispherectomy patient (40).

The internal capsule and the corticospinal tracts myelinate earlier than cortical and commissural tracts (41), and the splenium undergoes more postnatal axonal elimination than any other sector of the corpus callosum (42), a process that likely extends into the 6th or 7th postnatal month in human infants. Therefore, different biophysical mechanisms could affect the diffusion of water molecules in the corticospinal tracts and the splenium at different ages, namely density in splenium and myelination in the corticospinal tract, and thus lead to different directions of association with target behaviors. Considering the density of axons as the primary constraint on water diffusion in the splenium facilitates interpretation of the negative association with visual orienting latencies. A greater density of axons (a proportion of which will subsequently be selectively eliminated) should yield less radial diffusion and could reflect a less mature/efficient information processing system resulting in slower reaction times. However, this putative interpretation should be qualified by a growing literature that promotes extreme caution when making inferences about the underlying tissue structure that constrains water diffusion along and across fiber bundles (43). Future research using targeted imaging pulse sequences (41) has the potential to elucidate specific neuroanatomical mechanisms that underlie information processing during infancy.

Previous research has shown that visual orienting latencies are related to encoding speed in 4-month-olds (44), which subsequently predicts cognitive outcomes in preschool aged children (45). The current data reveal a disorder-specific deficit in visual orienting, such that infants who later express ASD

symptoms show significantly longer latencies than both high-risk-negative and low-risk infants. By extension, these data suggest that flexible and efficient visual orienting may also be important for typical patterns of social-cognitive development. Furthermore, the current results indicate that the functional coupling between visual orienting and white matter microstructure of the splenium observed in low-risk infants differs significantly from high-risk infants who later express ASD symptoms. More research is needed to explicate the precise neural mechanisms that underlie increased visual orienting latencies observed in infants who later express ASD, but the current data suggest that the functional efficiency of the splenium and the posterior heteromodal association areas may be critical.

With regard to oculomotor efficiency, or performance in the gap condition, the difference between low-risk and high-risk-ASD infants was quite large and statistically significant, which suggests a marked deficit in the saccade generating circuit (16;29). However, these behavioral differences were not explained by variability in the white matter microstructure in the corticospinal tracts (see Supplemental Figure 3), suggesting a more focused methodological approach is necessary to characterize the neural mechanism that mediates atypical oculomotor functioning in ASD. Of interest, the high-risk-negative and high-risk-ASD groups showed statistically equivalent gap latencies. When coupled with the trend toward a significant difference between high-risk-negative and low-risk infants ($p = 0.074$, $d = 0.41$), this pattern of results suggests that abnormal oculomotor functioning may be a familial marker of ASD (46).

Identifying infants at highest risk for ASD before the consolidation of syndromic features offers the possibility of implementing behavioral and other interventions during infancy that could reduce or prevent the manifestation of the full syndrome (47). Complementing and extending recent data suggesting early functional and structural brain abnormalities in infants who go on to develop ASD (48-49), the current behavioral findings have the potential to enhance early identification of individuals with ASD and to inform targeted interventions developed for the ASD prodrome. Of note, one recent study successfully altered visual orienting performance in 11 month-olds using several gaze-contingent attention training procedures administered during 5 lab visits over 15 days (50). One of the pre- and post-test procedures that tracked changes due to training was nearly identical to the gap/overlap procedure

used in the current study. Future research is needed to determine long term effects of modifying visual orienting patterns in infancy, specifically in relation to how training attention at specific time intervals during infancy might alter social-cognitive development.

Several limitations of the current study bear mention. First, we used the ADOS at 24 months to classify infants as either presenting ASD symptoms or not. It is currently unknown whether the toddlers who show ASD symptoms at 24 months will continue to present symptoms at 3 or 4 years of age. Additionally, increasing the number of high-risk infants would afford the opportunity to examine heterogeneity within the high-risk-ASD group, as well as potential compensatory mechanisms and heterogeneity in the high-risk-negative group. Lastly, radial and axial diffusivity and fractional anisotropy represent indices of white matter microstructure, but do not represent the organization of any one specific neurobiological component (e.g., myelin content). Multi-modal imaging will be imperative to definitively characterize the neural mechanisms that underlie the emergence of ASD symptoms.

Correspondence: Jed T. Elison, PhD, Division of Humanities and Social Science, California Institute of Technology, 1200 E. California Blvd., MC 228-77, Pasadena, CA 91125 (jelison@caltech.edu) or Joseph Piven, MD, Carolina Institute for Developmental Disabilities, University of North Carolina, Chapel Hill, NC 27599-7255 (jpiven@med.unc.edu).

Author Contributions

JTE and JP conceived the current project, had full access to all of the data, interpreted the data, wrote the manuscript, and take full responsibility for the integrity and accuracy of the data. The IBIS infant-sibling longitudinal design was conceived by JP in collaboration with HCH, LZ, RTS, HG, KNB, and SRD. The eye tracking task was designed by JTE and the eye tracking data were processed by JTE. GG, MS, SRD, SJP, RTS, ACE, and HCH designed the imaging protocol and oversaw the DTI data collection and DTI processing. JJW generated scalar diffusion measures. AME, LZ, HCH, KNB, and SJP oversaw the clinical/behavioral data collection. JSR and NJS contributed to the conceptual development of the study. All co-authors had full access to the data and edited the manuscript. The final revision was completed by JTE and JP.

Financial Disclosure: Dr. Evans is cofounder of and holds equity in Biospective, Inc., a company that performs image analysis for pharmaceutical companies; he has also received consulting fees from Johnson & Johnson and Pfizer within the last 36 months. Dr. Schultz reports receiving CME funding from Shire Pharmaceuticals, advisory panel funding from Seaside Therapeutics, and advisory panel funding from Roche. All other authors report no financial relationships with commercial interests.

Funding/Support: This research was supported by grants awarded to J.P. from NIH/NICHD (Autism Center of Excellence R01 #HD055741, #HD055741-S1; IDDRC, P30 #HD03110; and T32 HD40127), Autism Speaks, and the Simons Foundation. J.T.E. was supported by an NRSA award (5-T32-HD007376) from NICHD and aspects of this work contributed to his PhD dissertation. Further support was provided by the National Alliance for Medical Image Computing (NA-MIC), funded by the NIH through grant U54 EB005149. The sponsors/funders of this research played no role in the design and

conduct of this study, the collection, management, analysis, or interpretation of the data, nor the preparation, review or approval of the manuscript.
Additional Contributions: We wish to thank the IBIS children and families for their ongoing participation in this longitudinal study. We also wish to thank Ryan Scotton, Rachel G. Smith, Samir Das, and Penelope Kostopoulos for their effort; and Matt Mosconi, Keize Izuma, and Ralph Adolphs for their comments on the manuscript.

References

1. Klin A, Lin DJ, Gorrindo P, Ramsay G, Jones W: Two-year-olds with autism orient to non-social contingencies rather than biological motion. Nature 2009; 459(7244): 257-261.

2. Zwaigenbaum L, Bryson S, Rogers T, Roberts W, Brian J, Szatmari P: Behavioral manifestations of autism in the first year of life. Int J Dev Neurosci 2005; 23(2-3): 143-152.

3. Landa RJ, Holman KC, Garrett-Mayer E: Social and communication development in toddlers with early and later diagnosis of autism spectrum disorders. Arch Gen Psychiatry 2007; 64(7): 853-864.

4. Ozonoff S, Iosif AM, Baguio F, Cook IC, Hill MM, Hutman T, Rogers SJ, Rozga A, Sangha S, Sigman M, Steinfield MB, Young GS: A prospective study of the emergence of early behavioral signs of autism. J Am Acad Child Adolesc Psychiatry 2010; 49(3): 256-266.

5. Kagan J: Attention and psychological change in the young child. Science 1970; 170(3960): 826-832.

6. Posner MI, Petersen SE: The attention system of the human brain. Annu Rev Neurosci 1990; 13: 25-42.

7. Desimone R, Duncan J: Neural mechanisms of selective visual attention. Annu Rev Neurosci 1995; 18: 193-222.

8. Fan J, McCandliss BD, Fossella J, Flombaum JI, Posner MI: The activation of attentional networks. Neuroimage 2005; 26(2): 471-479.

9. Niogi S, Mukherjee P, Ghajar J, McCandless BD: Individual differences in distinct components of attention are linked to anatomical variations in distinct white matter tracts. Front Neuroanat 2010; 4(2): PMID: 20204143.

10. Corbetta M, Patel G, Shulman GL: The reorienting system of the human brain: from environment to theory of mind. Neuron 2008; 58(3): 306-324.

11. Vuilleumier P: How brains beware: neural mechanisms of emotional attention. Trends Cogn Sci 2005; 9(12): 585-594.

12. Leppanen JM, Nelson CA: Tuning the developing brain to social signals of emotion. Nat Rev Neurosci 2009; 10(1): 37-47.

13. Elsabbagh M, Volein A, Holmboe K, Tucker L, Csibra G, Baron-Cohen S, Bolton P, Charman T, Baird G, Johnson MH: Visual orienting in the early broader autism phenotype: disengagement and facilitation. J Child Psychol Psychiatry 2009; 50(5): 637-642.

~~14. Csibra G, Tucker LA, Volein A, Johnson MH: Cortical development and saccade planning: the ontogeny of the spike potential. Neuroreport 2000; 11(5): 1069-1073.~~

14. Putnam MC, Steven MS, Doron KW, Riggall AC, Gazzaniga MS: Cortical projection topography of the human splenium: hemispheric asymmetry and individual differences. J Cogn Neurosci 2010; 22(8): 1662-1669.

15. Duhamel, J-R, Colby CL, Goldberg ME: The updating of the representation of visual space in parietal cortex by intended eye movements. Science 1992; 255(5040): 90-92.

16. Dorris MC, Munoz DP: A neural correlate for the gap effect on saccadic reaction times in monkey. J Neurophysiol 1995; 73(6): 2558-2562.

17. Berument SK, Rutter M, Lord C, Pickles A, Bailey A: Autism screening questionnaire: diagnostic validity. Br J Psychiatry 1999; 175: 444-451.

18. Lord C, Rutter M, LeCouteur A: Autism Diagnostic Interview – Revised: a revised version of a diagnostic interview for caregivers of individuals with possible pervasive developmental disorders. J Autism Dev Disord 1994; 24(5): 659-685.

19. Mullen EM: Mullen Scales of Early Learning AGS Edition. Circle Pines, MN, American Guidance Services Publishing, 1995.

20. Lord C, Risi S, Lambrecht L, Cook EH, Leventhal BL, DiLavore PC, Pickles A, Rutter M: The autism diagnostic observation schedule-generic: a standard measure of social and communication deficits associated with the spectrum of autism. J Autism Dev Disord 2000; 30(3): 205-223.

28. Posner MI, Walker JA, Friedrich FJ, Rafal RD: Effects of parietal injury on covert orienting of attention. J Neurosci 1984; 4(7): 1863-1874.

29. Corbetta M: Frontoparietal cortical networks for directing attention and the eye to visual locations: identical, independent, or overlapping neural systems? Proc Natl Acad Sci USA 1998; 95(3): 831-838.

30. Goodlett CB, Fletcher PT, Gilmore JH, Gerig G: Group analysis of DTI fiber tract statistics with application to neurodevelopment. Neuroimage 2009; 45(1 Suppl): S133-S142.

31. Rueckert D, Sonoda LI, Hayes C, Hill DL, Leach MO, Hawkes DJ: Nonrigid registration using free-form deformations: application to breast MR images. IEEE Trans Med Imaging 1999; 18(8): 712-721.

32. Joshi S, Davis B, Jomier M, Gerig G: Unbiased diffeomorphic atlas construction for computational anatomy. Neuroimage 2004; 23(1 Suppl): S151-S160.

33. Salvador R, Pena A, Menon DK, Carpenter TA, Pickard JD, Bullmore ET: Formal characterization and extension of the linearized diffusion tensor model. Hum Brain Mapp 2005; 24(2): 144-155.

34. Alexander D, Pierpaoli C, Basser PJ, Gee J: Spatial transformations of diffusion tensor magnetic resonance images. IEEE Trans Med Imaging 2001; 20(11): 1131-1140.

35. Fletcher PT, Joshi S: Riemannian geometry for statistical analysis of diffusion tensor data. Signal Processing 2007; 87: 250-262.

36. Mori S, Wakana S, Nagae-Poetscher LM, van Zilj PCM: MRI Atlas of Human White Matter. Amsterdam, Elsevier, 2005.

37. Song SK, Sun SW, Ramsbottom MJ, Chang C, Russell J, Cross AH: Dysmyelination revealed through MRI as increased radial (but unchanged axial) diffusion of water. Neuroimage 2002; 17(3): 1429-1436.

38. Wake H, Lee PR, Fields RD: Control of local protein synthesis and initial events in myelination by action potentials. Science 2011; 333(6049): 1647-1651.

39. Madler B, Drabycz SA, Kolind SH, Whittall KP, MacKay AL: Is diffusion anisotropy an accurate monitor of myelination? Correlation of multicomponent T2 relaxation and diffusion tensor anisotropy in human brain. Magn Reson Imaging 2008; 26(7): 874-888.

40. Braddick O, Atkinson J, Hood B, Harkness W, Jackson G, Vargha-Khadem F: Possible blindsight in infants lacking one cerebral hemisphere. Nature 1992; 360: 461-463.

41. Deoni SCL, Dean DC, O'Muircheartaigh J, Dirks H, Jerskey BA: Investigating white matter development in infancy and early childhood using myelin water fraction and relaxation time mapping. Neuroimage 2012; 63(3): 1038-1053.

42. LaMantia AS, Rakic P: Axon overproduction and elimination in the corpus callosum of the developing rhesus monkey. J Neurosci 1990; 10(7): 2156-2175.

43. Wheeler-Kingshott CA, Cercignani M: About "axial" and "radial" diffusivities. Magn Reson Imaging 2009; 61(5): 1255-1260.

44. Frick JE, Colombo J, Saxon TF: Individual differences and developmental differences in disengagement of fixation in early infancy. Child Dev 1999; 70(3): 537-548.

45. Colombo J, Shaddy DJ, Richman WA, Maikranz JM, Blaga OM: The developmental course of habituation in infancy and preschool outcome. Infancy 2004; 5(1): 1-38.

46. Mosconi MW, Kay M, D'Cruz AM, Guter S, Kapur K, Macmillan C, Stanford LD, Sweeney JA: Neurobehavioral abnormalities in first-degree relatives of individuals with autism. Arch Gen Psychiatry 2010; 67(8): 830-840.

47. Dawson G: Early behavioral intervention, brain plasticity, and the prevention of autism spectrum disorder. Dev Psychopathol 2008; 20(3): 775-803.

48. Elsabbagh M, Mercure E, Hudry K, Chandler S, Pasco G, Charman T, Pickles A, Baron-Cohen S, Bolton P, Johnson MH; BASIS Team: Infant neural sensitivity to dynamic eye gaze is associated with later emerging autism. Curr Biol 2012; 22(4): 338-342.

49. Wolff JJ, Gu H, Gerig G, Elison JT, Styner M, Gouttard S, Botteron KN, Dager SR, Dawson G, Estes AM, Evans AC, Hazlett HC, Kostopoulos P, McKinstry RC, Paterson SJ, Schultz RT, Zwaigenbaum L, Piven J; IBIS Network: Differences in white matter fiber tract development present from 6 to 24 months in infants with autism. Am J Psychiatry 2012; 169(6): 589-600.

50. Wass S, Porayska-Pomsta K, Johnson MH: Training attentional control in infancy. Curr Biol 2011; 21(18): 1543-1547.

FIGURE LEGEND

Figure 1
Title: The Modified Gap Overlap Procedure.
During gap trials, a fixation image appeared in the center of a visual display for a variable duration; the central image then disappeared and was followed by a 250 millisecond temporal gap prior to the appearance of a target image in the peripheral visual field (all images subtended a visual angle of 5-7°, visual angle between images subtended 8-10°). During overlap trials, the central image remained present after the appearance of the peripheral target for the duration of the peripheral target presentation (i.e., 2 seconds).

Figure 2
Title: Regions of Interest (ROI) for Labelmap Seeding.
Panel A shows ROIs for the genu (yellow) and splenium (red) of the corpus callosum as applied to the centermost sagittal slice of the study atlas. Panel B shows axial ROIs for bilateral corticospinal white matter passing through the posterior limb of the internal capsule.

Figure 3
Title: Group Differences in Oculomotor and Visual Orienting Behavior
*Represents LSD pairwise group differences, $\alpha = 0.05$. In the gap condition, latencies for the 3 groups appear to represent a trend toward a familial marker model. In the overlap condition, latencies for the 3 groups conformed to a disorder-specific model of impairment (i.e., high-risk-ASD > high-risk-negative = low-risk). Error bars represent 1 standard deviation.

Figure 4
Title: Brain-Behavior Double Dissociation in 34 Low-Risk Seven-Month-Olds
4a) Results from a multiple regression analysis in which gap latencies account for a significant portion of variance in radial diffusivity in the left corticospinal tract, above and beyond age and overlap latencies. Regression lines within the scatterplots represent the zero-order correlation between radial diffusivity in the left corticospinal tract and overlap latencies (full black circles; $r = -0.128$, $p = 0.472$) and gap latencies (open black circles; $r = 0.592$, $p < 0.001$), respectively. See Supplemental Figure 1 for results on the right corticospinal tract. 4b) Results from a multiple regression analysis in which overlap latencies account for a significant portion of variance in radial diffusivity in the splenium, above and beyond age and gap latencies. Regression lines within the scatterplots represent the zero-order correlation between radial diffusivity in the splenium and overlap latencies (full black circles; $r = -0.499$, $p = 0.003$) and gap latencies (open black circles; $r = 0.006$, $p = 0.975$), respectively.

Figure 5
Title: Functional Coupling between Visual Orienting and the Splenium
Group membership significantly moderates the association between individual differences in radial diffusivity in the splenium and average saccadic latency in the overlap condition.

Table 1. Participant Characterization

Characteristic	low-risk (n = 41)		high-risk-neg (n = 40)		high-risk-ASD (n = 16)		ANOVA		pairwise group differences: high-risk-ASD & low-risk	pairwise group differences: high-risk-ASD & high-risk-neg
							$F_{(2,94)}$	*p*	*p*	*p*
Sex (M:F)[1]	24:17		20:20		11:5					
	mean	*sd*	mean	*sd*	mean	*sd*				
1st visit age (months)	7.1	*0.8*	7.0	*0.8*	7.2	*1.0*	0.51	0.604	0.636	0.340
Mullen[2]										
ELC	107.8	*10.9*	105.0	*11.7*	101.4	*12.7*	1.81	0.170	0.066	0.300
NVDQ	107.4	*15.1*	106.5	*18.5*	105.5	*11.8*	0.08	0.919	0.692	0.833
VDQ	104.2	*15.9*	97.0	*17.4*	93.8	*19.5*	2.79	0.067	0.044	0.535
Vis. Rec t score	53.4	*7.6*	52.8	*8.0*	52.6	*7.3*	0.10	0.904	0.725	0.957
Clinical visit age (months)	24.8	*0.8*	25.0	*1.1*	25.4	*1.9*	1.57	0.215	0.081	0.200
ADOS[3]										
SA Subscale	1.9	*1.9*	2.0	*1.4*	11.9	*4.1*	123.0	< 0.001	< 0.001	< 0.001
RRB Subscale	0.3	*0.7*	0.6	*0.9*	2.6	*2.0*	25.2	< 0.001	< 0.001	< 0.001
Total	2.2	*2.1*	2.6	*1.8*	14.6	*5.5*	114.6	< 0.001	< 0.001	< 0.001

[1]According to a Fisher's exact test, the sex ratio did not significantly differ by risk status, $p = 0.427$.
[2]Mullen Scales of Early Learning: ELC = Early Learning Composite Score (composite of the receptive language, expressive language, fine motor, and visual reception standard scores); NVDQ = Nonverbal Developmental Quotient (average age equivalent scores for the fine motor and visual reception subscales divided by chronological age multiplied by 100); VDQ = Verbal Developmental Quotient (average age equivalent scores for the receptive language and expressive language subscales divided by chronological age multiplied by 100); Vis. Reception t score = Visual Reception standardized score.

[3]Autism Diagnostic Observation Scale (ADOS) was conducted when the child was between 23.6 and 32.7 months of age. The ADOS yields a social-affect subscale score and a restricted and repetitive behavior subscale score. The total ADOS score is the sum of the two subscales. All children in the ASD group met diagnostic criteria for a provisional autism spectrum diagnosis according to the ADOS.

Table 2: Summary of Performance in the Gap Overlap Paradigm

							ANOVA		pairwise group differences			
									high-risk-ASD & low-risk		high-risk-ASD & high-risk-neg	
Characteristic	**low-risk (n = 41)**		**high-risk-neg (n = 40)**		**high-risk-ASD (n = 16)**		$F_{(2,94)}$	*p*	*p*	*d*[7]	*p*	*d*[7]
	mean	*sd*	mean	*sd*	mean	*sd*						
valid overlap trials[1]	11.9	*6.0*	13.5	*5.9*	11.2	*4.1*	1.30	0.277				
valid gap trials[1]	12.9	*5.7*	14.1	*5.1*	12.1	*4.9*	0.93	0.400				
overlap_saccade rate[2]	331	*110*	322	*139*	383	*161*	1.28	0.283				
gap_saccade rate[2]	371	*127*	343	*150*	362	*185*	0.36	0.697				
overlap_latency[3]	412.6	*59.0*	404.9	*72.5*	454.6	*62.2*	3.42	0.037	0.032	0.71	0.012	0.73
gap_latency[3]	271.4	*36.9*	287.5	*42.1*	298.4	*42.9*	3.14	0.048	0.025	0.71	0.362	0.26
overlap_CoV[4]	0.276	*0.10*	0.292	*0.08*	0.303	*0.09*	0.60	0.551				
gap_CoV[4]	0.172	*0.08*	0.195	*0.10*	0.190	*0.09*	0.74	0.480				
gap-effect[5]	141	*55.3*	117	*64.1*	156	*56.3*	3.00	0.055	0.390	0.27	0.029	0.64
late or no saccade[6]	1.20	*1.57*	1.83	*2.12*	2.13	*2.00*	1.85	0.163				

[1]Mean and standard deviation of valid overlap trials and valid gap trials.
[2]Average saccade rate/velocity for overlap trials and gap trials, units = degrees/second. A minimum velocity threshold was set at 80°/sec.
[3]Average latency to initiate saccade toward the lateral target in the overlap condition and the gap condition in ms.
[4]Coefficient of Variation (CoV) for saccade latencies in the overlap condition and the gap condition. The CoV is a standardized index of dispersion or variability and is derived by estimating the ratio of the standard deviation to the mean for each individual (σ/μ).
[5]The gap-effect value represents the difference between average overlap latency and average gap latency in ms. While a common metric extracted from this task, the gap-effect value violates the assumption of pure insertion, as there are likely more than 1 cognitive/neural components active in one condition and not the other.
[6]"Late or no saccade" represents the number of trials that were excluded because the infant failed to initiate a saccade toward the lateral target between 100 and 1000 ms after the onset of the lateral target. This value also includes saccades that were more than 2 standard deviations from the mean, which always fell at the upward end of the distribution.
[7]Effect size based on Cohen's *d*, using pooled variance as the denominator.

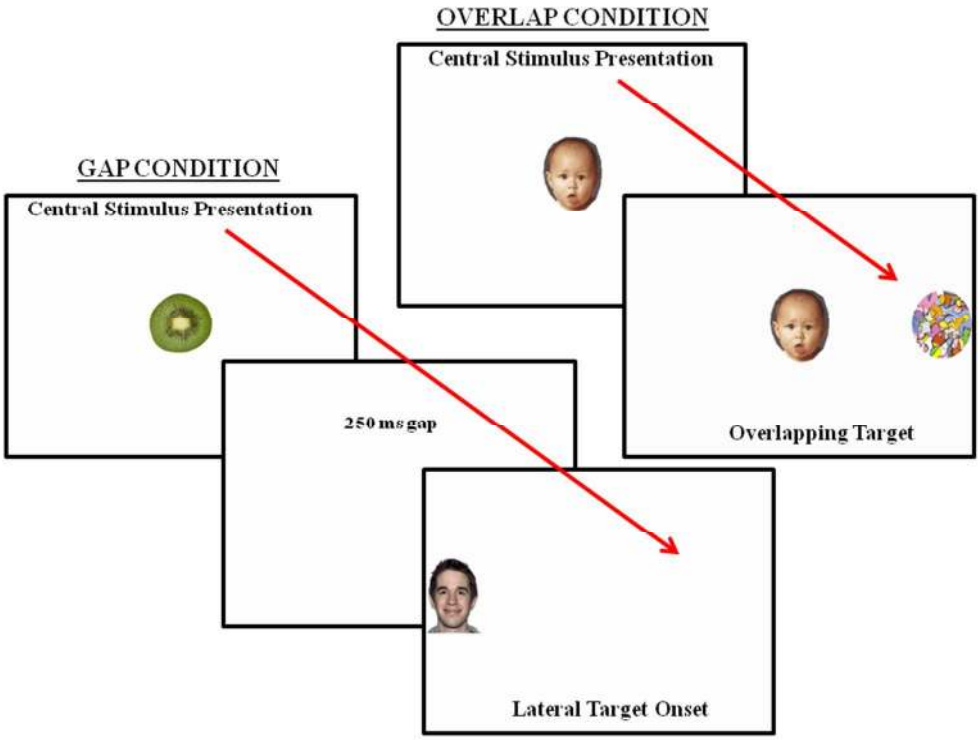

Title: The Modified Gap Overlap Procedure.
During gap trials, a fixation image appeared in the center of a visual display for a variable duration; the central image then disappeared and was followed by a 250 millisecond temporal gap prior to the appearance of a target image in the peripheral visual field (all images subtended a visual angle of 5-7°, visual angle between images subtended 8-10°). During overlap trials, the central image remained present after the appearance of the peripheral target for the duration of the peripheral target presentation (i.e., 2 seconds).

254x190mm (96 x 96 DPI)

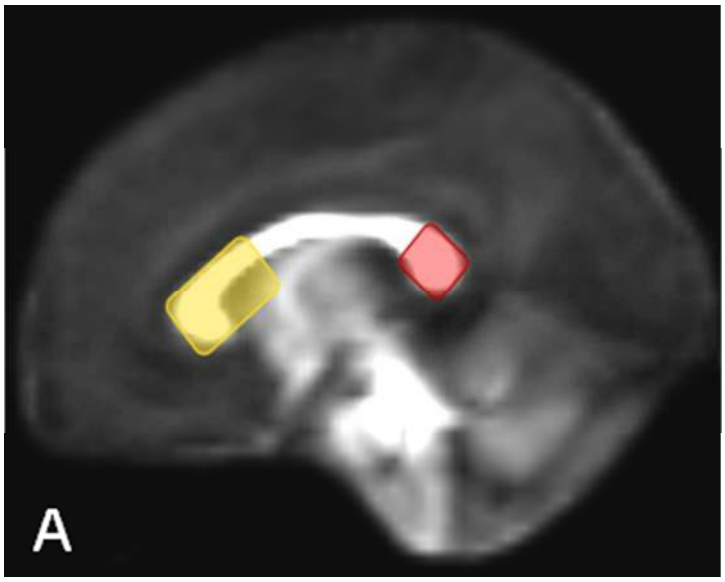

Title: Regions of Interest (ROI) for Labelmap Seeding.
Panel A shows ROIs for the genu (yellow) and splenium (red) of the corpus callosum as applied to the centermost sagittal slice of the study atlas.
94x75mm (96 x 96 DPI)

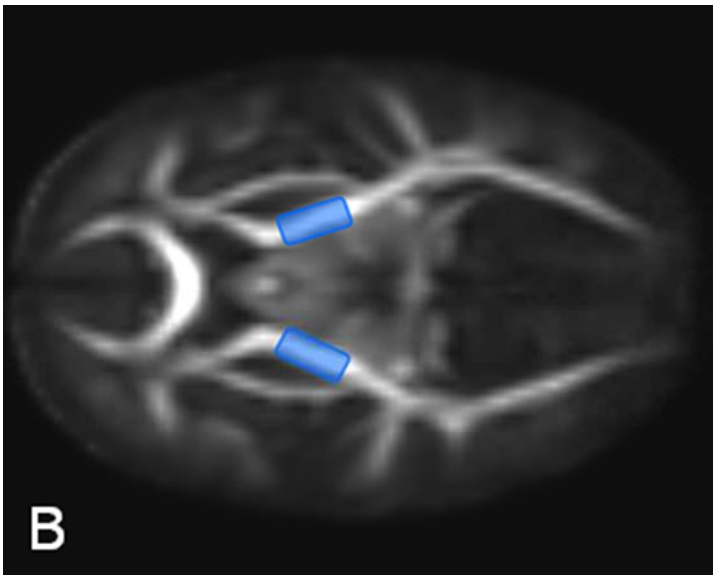

Title: Regions of Interest (ROI) for Labelmap Seeding.
Panel B shows axial ROIs for bilateral corticospinal white matter passing through the posterior limb of the internal capsule.
93x75mm (96 x 96 DPI)

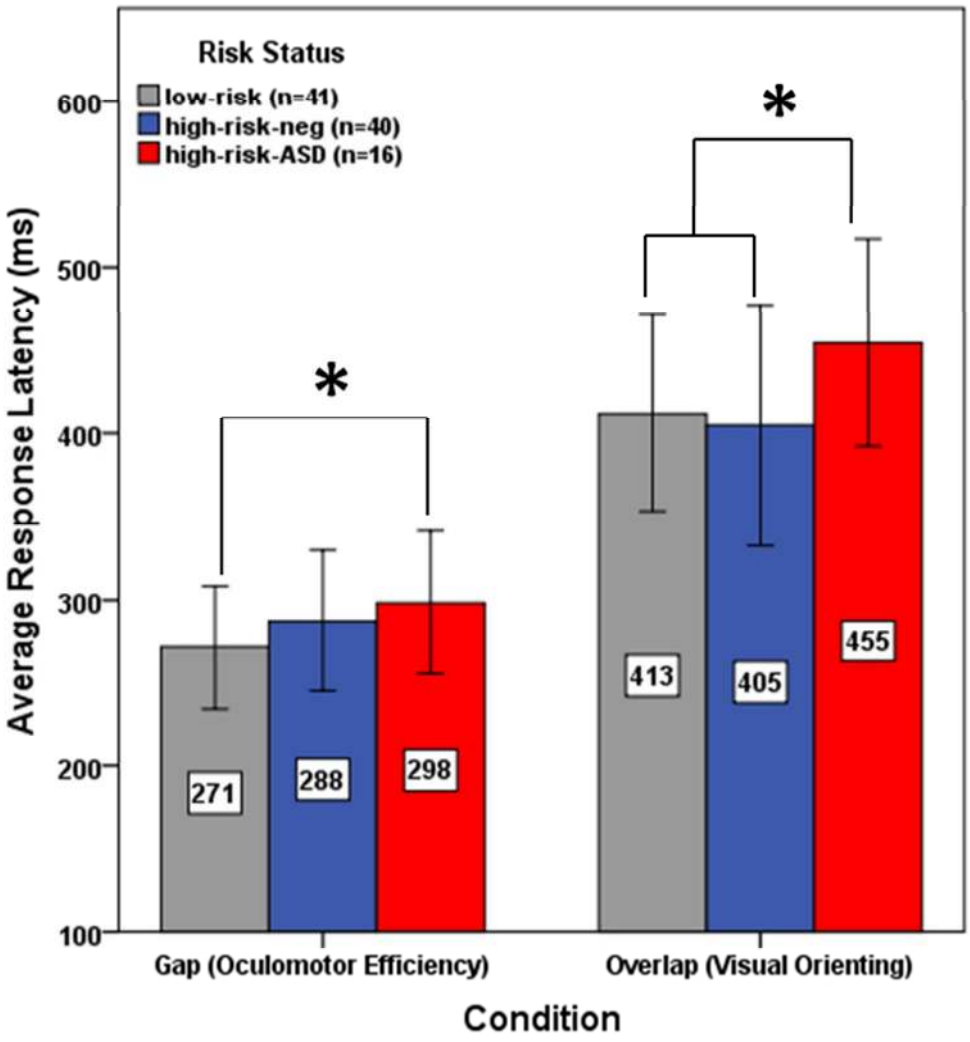

Title: Group Differences in Oculomotor and Visual Orienting Behavior
*Represents LSD pairwise group differences, α = 0.05. In the gap condition, latencies for the 3 groups appear to represent a trend toward a familial marker model. In the overlap condition, latencies for the 3 groups conformed to a disorder-specific model of impairment (i.e., high-risk-ASD > high-risk-negative = low-risk). Error bars represent 1 standard deviation.

175x184mm (96 x 96 DPI)

a

Multiple regression analysis for left corticospinal tract + gap

Model	R	R^2	R^2change	Fchange	Sig. F change
1	0.167[a]	0.028	0.016	0.522	0.475
2	0.717[b]	0.514	0.486	30.041	0.000

[a] predictors: (constant), age, overlap latency

[b] predictors: (constant), age, overlap latency, gap latency

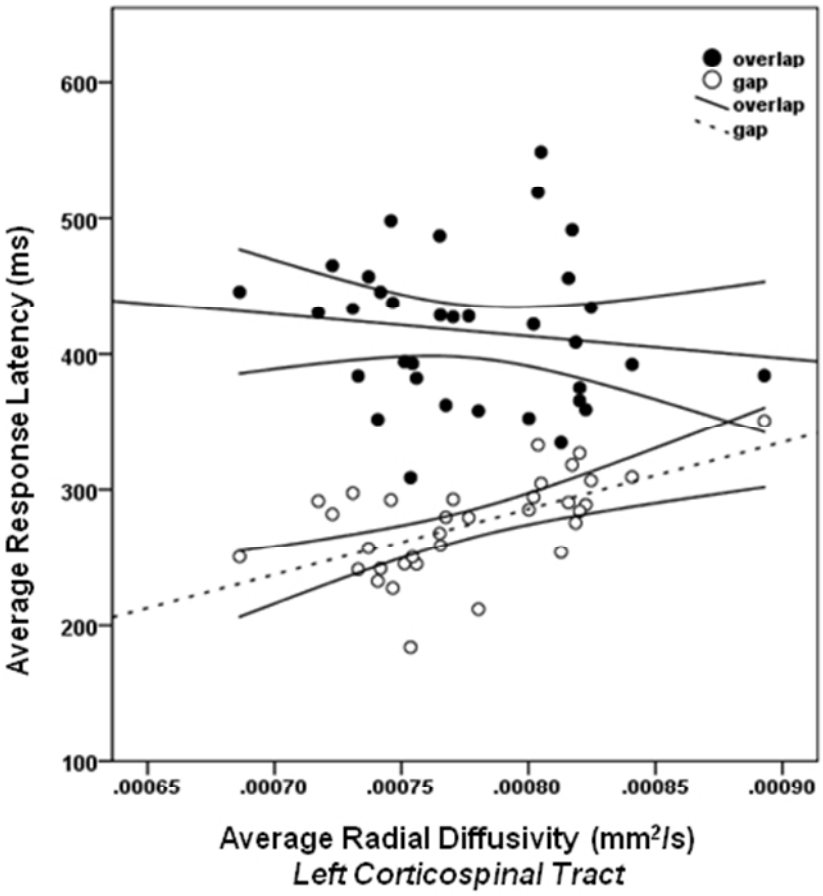

Title: Brain-Behavior Double Dissociation in 34 Low-Risk Seven-Month-Olds

4a) Results from a multiple regression analysis in which gap latencies account for a significant portion of variance in radial diffusivity in the left corticospinal tract, above and beyond age and overlap latencies. Regression lines within the scatterplots represent the zero-order correlation between radial diffusivity in the left corticospinal tract and overlap latencies (full black circles; r = -0.128, p = 0.472) and gap latencies (open black circles; r = 0.592, p < 0.001), respectively. See Supplemental Figure 1 for results on the right corticospinal tract.

124x171mm (96 x 96 DPI)

b

Multiple regression analysis for splenium + overlap

Model	*R*	R^2	R^2change	*F*change	Sig. *F* change
1	0.098[a]	0.010	0.010	0.151	0.860
2	0.554[b]	0.307	**0.297**	12.855	**0.001**

[a] *predictors: (constant), age, gap latency*

[b] *predictors: (constant), age, gap latency, overlap latency*

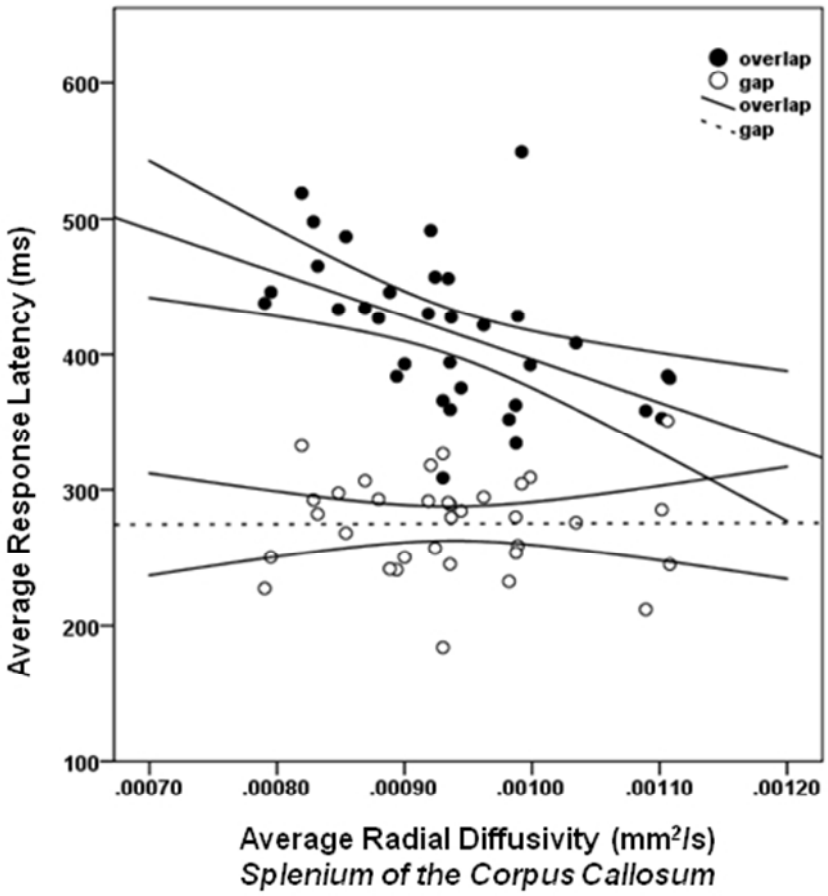

Title: Brain-Behavior Double Dissociation in 34 Low-Risk Seven-Month-Olds

4b) Results from a multiple regression analysis in which overlap latencies account for a significant portion of variance in radial diffusivity in the splenium, above and beyond age and gap latencies. Regression lines within the scatterplots represent the zero-order correlation between radial diffusivity in the splenium and overlap latencies (full black circles; r = -0.499, p = 0.003) and gap latencies (open black circles; r = 0.006, p = 0.975), respectively.

124x171mm (96 x 96 DPI)

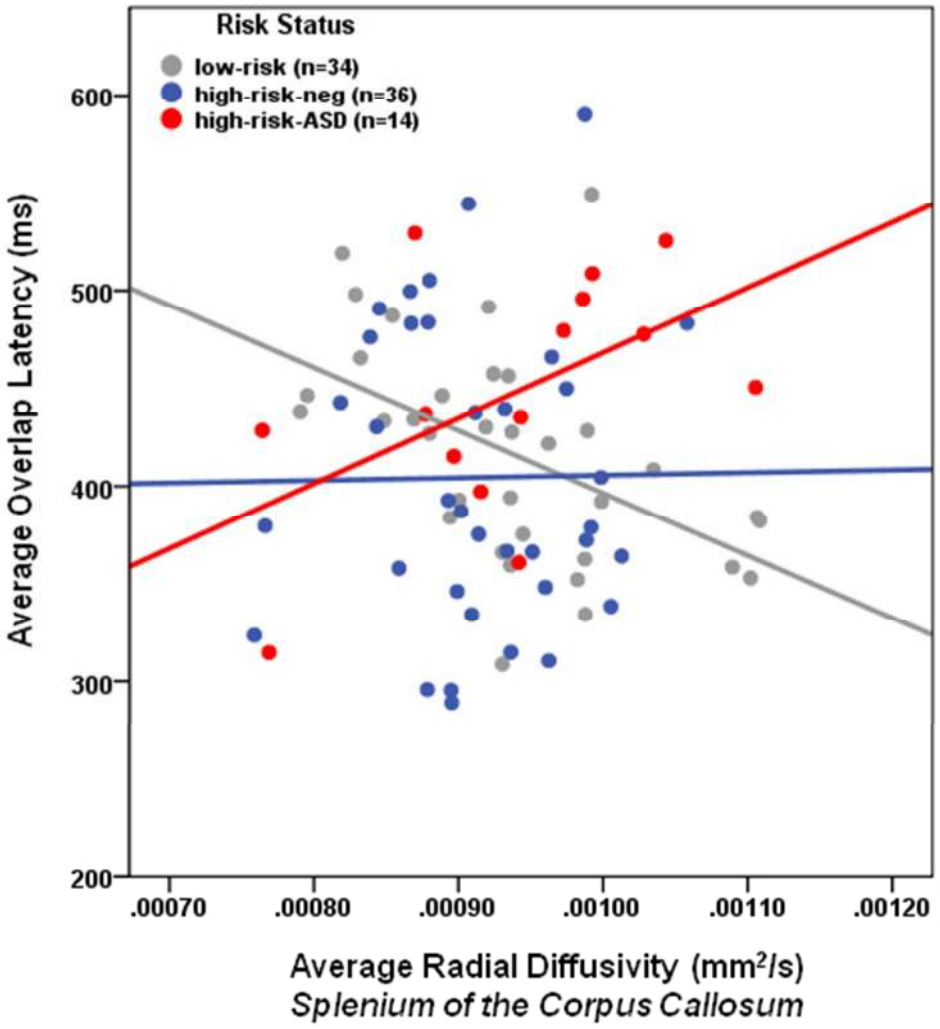

Title: Functional Coupling between Visual Orienting and the Splenium
Group membership significantly moderates the association between individual differences in radial diffusivity in the splenium and average saccadic latency in the overlap condition.

128x137mm (96 x 96 DPI)